Photochemistry of Locally Excited and Intramolecular Charge Transfer States of (*E*)-4-Cyano-4′-(pentamethyldisilanyl)stilbene

**Gui Liu, Ladislau Heisler, Lin Li, and Mark G. Steinmetz***

Contribution from the Department of Chemistry, Marquette University, P.O. Box 1881, Milwaukee, Wisconsin 53201-1881

Received July 1, 1996[⊗]

Abstract: The photophysical properties and photochemistry of (*E*)-4-cyano-4′-(pentamethyldisilanyl)stilbene ((*E*)-**3**) and the corresponding monosilylated stilbene (*E*)-**5** have been studied. Solvatochromic plots of (*E*)-**3** show separate slopes for ether solvents and halocarbons. The emission in ethers is assigned to an LE state of similar polarity to that of (*E*)-**5**. In halocarbons a more polar intramolecular charge transfer (CT) state apparently contributes to the emission. This component is completely quenched by nucleophilic ethers. In contrast to (*E*)-**5**, Φ_f and $\Phi(E,Z)$ of (*E*)-**3** strongly decrease in CH_3CN, consistent with the solvent polarity induced LE → CT process and nucleophilic quenching of the CT state by solvent. Alcohols also quench Φ_f and $\Phi(E,Z)$ with similar Stern−Volmer constants, linking the two processes to the same state (LE). Such quenching results in formation of (*E*)-4′-(hydrodimethylsilyl)-4-cyanostilbene (**4**) by regioselective nucleophilic cleavage of the Si−Si bond, according to deuterium labeling studies. Double reciprocal plots of $\Phi^{-1}(SiH)$ vs $[ROH]^{-1}$ are consistent with both the LE and CT states being quenched by ROH with the latter state giving (*E*)-**4**. Quadratic behavior for MeOH in CH_2Cl_2 is ascribed to a solvent polarity promoted LE → CT process with a rate constant ∝ [MeOH], in accord with the linear relation of $E_T(30)$ vs ln [MeOH] above 0.3 M MeOH. The quadratic behavior disappears in *tert*-amyl alcohol, which has the same $E_T(30)$ as CH_2Cl_2. Results for MeOH in pentane suggest the LE and CT states have similar energies and interconvert.

Introduction

Photolyses of (*p*-(trifluoromethyl)phenyl)pentamethyldisilane (**1**) and 1-(*p*-cyanophenyl)-2-(pentamethyldisilanyl)cyclopentene (**2**) in alcohols produce aryl- and arylcyclopentenyl-substituted hydrodimethylsilanes.[1,2] These hydrodimethylsilanes are considered as being formed from cleavage of an electron-deficient
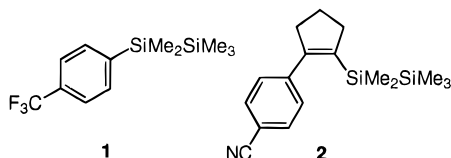
Si−Si bond through regioselective nucleophilic attack by alcohol at the terminal trimethylsilyl group. Such cleavage is accompanied by proton transfer from alcohol to the silyl group attached to the arene, since SiD-labeled hydrosilanes are observed on photolysis with O-deuterated alcohols. This photoprocess has experimental support as occurring in an intramolecular charge transfer (CT) state or twisted intramolecular CT (TICT) state,[1,2] which for **1** and **2** is the lowest energy excited singlet according to fluorescence studies. In these systems the direction of the electron transfer is from the disilanyl group to the photoexcited arene electron acceptor.[3] For arylcyclopentenyldisilane **2** the fluorescent CT state has been directly linked to the formation of the hydrodimethylsilane photoproduct through plots of $\Phi_f°/\Phi_f$ versus [MeOH] and $1/\Phi$(hydrosilane) versus $1/$[MeOH], which are linear with identical $k_q\tau$.[2] In contrast, a quadratic plot of $1/\Phi$(hydrosilane) versus $1/$[EtOH] in hexane has been reported for **1**.[1] The quadratic behavior has been ascribed to a solvent polarity dependent rate constant for electron transfer.[1]

The major photoproducts of **1** in alcohols are silyl ethers rather than the hydrodimethylsilane. These silyl ethers are produced from alcohol addition to a silene intermediate formed via [1,3] shift of the terminal trimethylsilyl group to an ortho position of the aromatic ring.[1] Whereas the locally excited (LE) state of **1** has been assigned as the reactive state,[1] photochemical studies of the parent compound, phenylpentamethyldisilane, have led to the opposite conclusion, that the CT state rather than the LE state undergoes the [1,3-Si] shift.[3−7] The [1,3-Si] shift is not observed with **2**.[2] Instead, a tricyclic product is produced by a potential mechanism involving homolytic Si−Si cleavage, radical cyclization, and disproportionation of the silyl radical pair. Both the LE and the CT states have been tentatively proposed as the reactive states.[2] Laser flash photolysis studies of phenylpentamethyldisilane indicate that homolytic Si−Si cleavage is a triplet excited state photoprocess of aryldisilanes, and the intersystem crossing is promoted by polar solvents.[8]
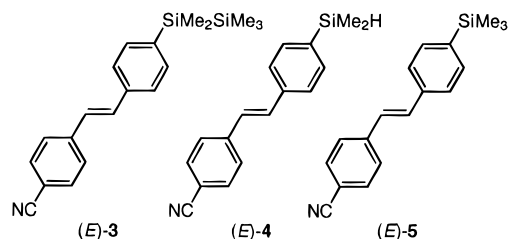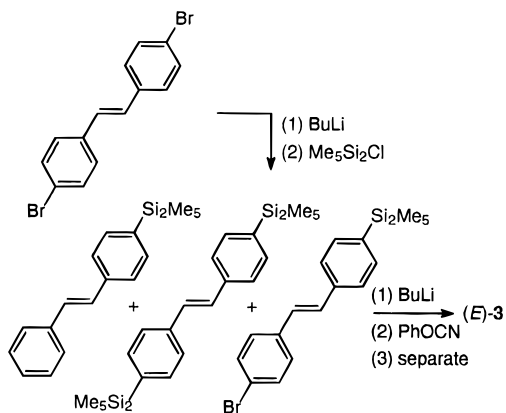

In this paper we report on the photochemistry of the disilanyl electron donor-substituted stilbene (*E*)-**3**. In addition to produc-

(1) Kira, M.; Miyazawa, T.; Sugiyama, H.; Yamaguchi, M.; Sakurai, H. *J. Am. Chem. Soc.* **1993**, *115*, 3116.

(2) Steinmetz, M. G.; Yu, C.; Li, L. *J. Am. Chem. Soc.* **1994**, *116*, 932.

(3) Steinmetz, M. G. *Chem. Rev.* **1995**, *95*, 1527.

(4) Shizuka, H.; Obuchi, H.; Ishikawa, M.; Kumada, M. *J. Chem. Soc., Faraday Trans. 1* **1984**, *80*, 383.

(5) Shizuka, H.; Hiratsuka, H. *Res. Chem. Intermed.* **1992**, *18*, 131.

(6) Shizuka, H. *Pure Appl. Chem.* **1993**, *65*, 1635.

(7) Shizuka, H.; Okazaki, K.; Tanaka, M.; Ishikawa, M.; Sumitani, M.; Yoshihara, K. *Chem. Phys. Lett.* **1985**, *113*, 89.

(8) Leigh, W. J.; Sluggett, G. W. *J. Am. Chem. Soc.* **1993**, *115*, 7531.

Scheme 1

Figure 1. Fluorescence of 1.0×10^{-4} M (*E*)-**3** in various solvents: pentane (—), Bu$_2$O (- - -), Et$_2$O (•••), CHCl$_3$ (•—•), CH$_2$Cl$_2$ (••—••), THF (bold line).

ing hydrodimethylsilane (*E*)-**4** in alcohols, stilbene (*E*)-**3** fluoresces and undergoes efficient *E,Z* photoisomerization. Since the latter two photoprocesses are quenched by alcohols, the kinetics of Stern–Volmer quenching can be compared to the kinetics of formation of hydrodimethylsilane (*E*)-**4** in order to assign the excited states involved in each process. In addition, the quantum yields for hydrosilane formation as a function of alcohol concentration are used to investigate the solvent polarity dependence of the LE to CT conversion previously reported for **1**.

Results

Synthesis of (*E*)-4-Cyano-4′-(pentamethyldisilanyl)stilbene (*E*)-3, Preparative Photolysis, Photoproducts, and Deuterium Labeling. Stilbene (*E*)-**3** was synthesized from (*E*)-4,4′-dibromostilbene (Scheme 1). Lithiation and treatment with chloropentamethyldisilane produced a mixture of 4-bromo-4′-disilanylstilbene and mono- and bis(disilanyl)stilbenes. This mixture was subjected to cyanation, column chromatographic separation, and purification by crystallization to obtain (*E*)-**3**. Stilbene (*E*)-**3** and its photomixtures had to be protected from ambient light.

Preparative photolysis of 6×10^{-3} M stilbene (*E*)-**3** in MeOH utilizing Pyrex filtered light of a 450-W medium-pressure mercury lamp gave, after chromatographic separation, 15% (*Z*)-**3**, 34% of an *E,Z* mixture of (hydrodimethylsilyl)stilbenes **4**, and 42% recovered reactant. In addition, an *E,Z* mixture of 4-cyano-4′-(methoxydimethylsilyl)stilbenes were detected in ca. 11% combined yield by GC-MS; the yields of these methoxysilanes were negligible at low conversions.

Preparative photolyses with 0.01 M (*E*)-**3** in pure MeOD resulted in 100% monodeuteration of (hydrodimethylsilyl)-stilbene (*E*)-**4**, according to GC-MS analysis of the parent ion and the M − 15 fragment ion. The deuterium was incorporated exclusively as SiD according to ^{2}H NMR analysis, and no detectable SiH was observed by ^{1}H NMR. For 5 M MeOD in pentane as the solvent GC-MS analyses showed 86% and 91% monodeuteration, as calculated from the parent and M − 15 ions, respectively, and 94% and 100% monodeuteration of **4** was found for 5 M MeOD in CH$_2$Cl$_2$ as the solvent.

Fluorescence Studies. Fluorescence spectra of (*E*)-**3** in the solvents pentane, (*n*-Bu)$_2$O, Et$_2$O, THF, CHCl$_3$, and CH$_2$Cl$_2$ are shown in Figure 1 and the data are summarized in Table 1. The structured fluorescence of (*E*)-**3** observed at 382 nm in pentane shifts to longer wavelengths with increasing polarity of the solvent. For halogenated solvents the shifts are larger than for the ethers and significant loss of structure is observed for CHCl$_3$ and CH$_2$Cl$_2$. The emission in CH$_3$CN is too weak to determine the maximum reliably. A plot (not shown) of the Stokes shift $\nu_a - \nu_f$ versus solvent polarity parameter $\Delta f = (\epsilon -$
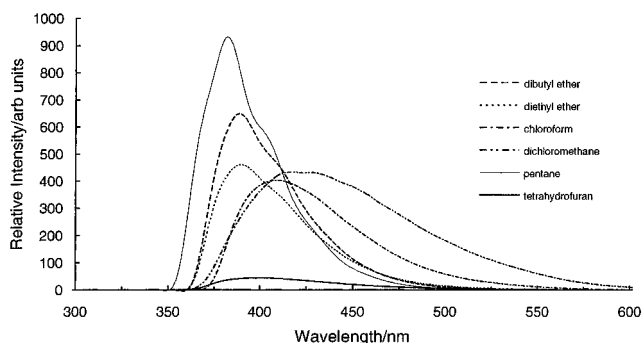
$1)/(2\epsilon + 1) - (n^2 - 1)/(2n^2 + 1)$ (eq 1), where ϵ and n are solvent dielectric constant and refractive index (eq 2),[9] gives $m = 4000 \pm 994$ cm^{-1}/Δf ($R^2 = 0.9436$) for pentane plus (*n*-Bu)$_2$O, Et$_2$O, THF. The chlorinated solvents show a separate linear correlation with slope $m = 9120 \pm 1810$ ($R^2 = 0.9808$) cm^{-1}/Δf and an intercept nearly the same as the ethers. The slopes of such plots are proportional to the square of the difference between ground and excited state dipole moments, $\Delta\mu^2$. Assuming the same molecular dimensions apply to (*E*)-**3** as for 4-cyano-4′-(dimethylamino)stilbene (DCS, $\rho = 5.43$ Å[10a]), the calculated $\Delta\mu$ are 8 D and 12 D.

Better linearity is found when the fluorescence maxima in Table 1 are plotted against $(\epsilon - 1)/(\epsilon + 2)$ according to eq 2[9b,10b] (Figure 2), in order to take into account polarization effects. The term $0.5(n^2 - 1)/(n^2 + 2) \approx 0.11$ and is approximately constant for the solvents of Table 1. The linear

$$\nu_a - \nu_f = \frac{2\Delta\mu^2}{hc\rho^3}\left(\frac{\epsilon - 1}{2\epsilon + 1} - \frac{n^2 - 1}{2n^2 + 1}\right) + \text{constant} \quad (1)$$

$$\nu_f = -\frac{2}{hc\rho^3}\left[(\mu_e° - \mu g)\mu_e°\left(\frac{\epsilon - 1}{\epsilon + 2}\right) - \frac{1}{2}(\mu_e° - \mu g)^2\left(\frac{n^2 - 1}{n^2 + 2}\right)\right] + \text{constant}' \quad (2)$$

correlation for pentane plus ethers has slope $m = -2440 \pm 356$ ($R^2 = 0.9794$) and the halogenated solvents give a separate slope $m = -4270 \pm 246$ ($R^2 = 0.9983$). From the slopes $\mu_e°(\mu_e° - \mu_g) = 39$ and 68 D^2, which afford lower limit estimates of the dipole moments $\mu_e°$ of the solvent-free, emissive excited states of 6 and 8 D, calculated by neglecting the ground state dipole moment μ_g.

The solvent polarity induced shifts in the fluorescence maxima of (*E*)-**5** for the series of solvents pentane, (*n*-Bu)$_2$O, Et$_2$O, CH$_2$Cl$_2$, and CH$_3$CN give a linear plot of ν_f versus $(\epsilon - 1)/(\epsilon + 2)$ (eq 2) with slope $m = -2299 \pm 225$ ($R^2 = 0.9859$) (Figure 2). Unlike (*E*)-**3** strong deviation of CH$_2$Cl$_2$ from the correlation is not observed. The slope with $\rho = 5.43$ Å as with DCS (vide supra) gives $\mu_e°(\mu_e° - \mu_g) = 37$ D^2, and the lower limit estimate of $\mu_e°$ is 6 D for $\mu_g = 0$.

Quantum yields of fluorescence of disilane (*E*)-**3** and monosilane (*E*)-**5** in pentane, CH$_2$Cl$_2$ and CH$_3$CN as solvents are summarized in Table 2. In the case of (*E*)-**3** a 30−50-fold decrease is observed for CH$_3$CN compared to CH$_2$Cl$_2$ or pentane

(9) (a) Rettig, W. *Angew. Chem., Int. Ed. Engl.* **1986**, *25*, 971 and references cited therein. (b) Liptay, W. *Z. Naturforsch.* **1965**, *20a*, 1441.
(10) (a) Lapouyade, R.; Czeschka, K.; Majenz, W.; Rettig, W.; Gilabert, E.; Rulliere, C. *J. Phys. Chem.* **1992**, *96*, 9643 and references cited therein. (b) Létard, J.-F.; Lapouyade, R.; Rettig, W. *J. Am. Chem. Soc.* **1993**, *115*, 2441.

Table 1. Absorption (λ_a) and Emission (λ_f) Maxima of (*E*)-**3** and (*E*)-**5**

| | | | disilane (*E*)-**3** | | | monosilane (*E*)-**5** | |
solvent	$E_T(30)$	$\Delta f(\epsilon,n)$	$(\epsilon - 1)/(\epsilon + 2)$	λ_a/nm	ϵ/M^{-1} cm^{-1}	λ_f/nm	λ_a/nm	λ_f/nm
pentane	31.0	0.001	0.219	329	45 000	382	324	374
Bu$_2$O	33.0	0.096	0.409	331	46 100	388	326	379
Et$_2$O	34.5	0.167	0.516	330	41 800	390	324	380
THF	37.4	0.210	0.687	332	46 400	400	nd^a	nd
CCl$_4$	32.4	0.010	0.291	334	41 966	392	nd	nd
CHCl$_3$	39.1	0.148	0.559	335	46 000	409	nd	nd
CH$_2$Cl$_2$	40.7	0.217	0.726	333	37 600	423	328	391
CH$_3$CN	45.6	0.305	0.921	330	46 100	br^b	325	397

^{a} Not determined. ^{b} Very weak, broad emission (370−625 nm).
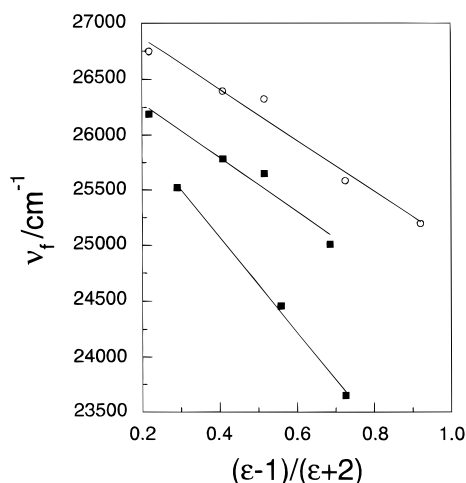
Figure 2. Solvatochromic plot of ν_f vs $(\epsilon - 1)/(\epsilon + 2)$ for (*E*)-**3** (■) and (*E*)-**5** (○).

Table 2. Quantum Yields for Fluorescence and *E,Z* Isomerization of (*E*)-**5** and (*E*)-**3** in Various Solvents and for Formation of (*Z*)-**3** and (*E*)-**4** from (*E*)-**3** in 5 M ROH
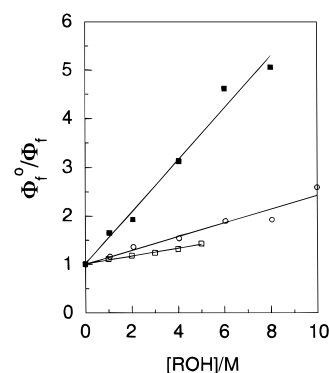
| | monosilane (*E*)-**5** | | disilane (*E*)-**3** | | | |
solvent	Φ_f	$\Phi(E,Z)$	Φ_f	$\Phi(E,Z)$	$\Phi(E,Z)^a$	$\Phi(SiH)^a$
pentane	0.031	0.38	0.10	0.41	0.28	0.019
CH$_2$Cl$_2$	0.023	0.40	0.20	0.55	0.11	0.022
					(0.40)^b	(0.0070)^b
CH$_3$CN	0.016	0.39	0.003	0.012	0.012	0.014

^{a} 5 M MeOH. ^{b} In parentheses, 5 M *tert*-amyl alcohol.

as solvents, whereas the monosilane (*E*)-**5** shows only small variations in emission efficiency as a function of solvent polarity.

Quenching of the steady-state fluorescence of 0.01 M (*E*)-**3** by binary mixtures of MeOH in pentane and CH$_2$Cl$_2$ and by *tert*-amyl alcohol (TAA) in CH$_2$Cl$_2$ was studied in detail so that Stern−Volmer quenching constants could be obtained for comparison to those of the photoproducts (vide infra). Unlike MeOH, which has $E_T(30) = 55.4$ kcal mol^{-1} indicative of substantially higher polarity than CH$_2$Cl$_2$ ($E_T(30) = 40.7$ kcal mol^{-1}), TAA has an $E_T(30) = 41.1$ kcal mol^{-1} nearly identical to that of CH$_2$Cl$_2$.[11] Thus, the concentration of TAA could be varied without modifying the polarity of the bulk solvent. For both MeOH and TAA, plots of relative quantum yields of fluorescence, Φ_f°/Φ_f, versus [ROH] displayed good linearity with slopes $k_q\tau$, where k_q is the apparent bimolecular rate constant for quenching of excited state with lifetime τ (Figure 3 and Table 3). The fluorescence of monosilylstilbene (*E*)-**5** was also quenched by MeOH in pentane with $k_q\tau = 0.15 \pm 0.02$ ($R^2 = 0.9780$).

Singlet excited state lifetimes were measured by monitoring the fluorescence of (*E*)-**3** using standard nanosecond single

(11) Reichardt, C. *Solvents and Solvent Effects in Organic Chemistry*; VCH Publishers: Weinheim, 1988.

Figure 3. Quenching of fluorescene of (*E*)-**3** by MeOH in pentane (○), by MeOH in CH$_2$Cl$_2$ (■), and by TAA in CH$_2$Cl$_2$ (□).

photon counting techniques.[12] Although fits to double exponential decays were attempted, in general satisfactory fits were only obtained for monoexponential decays (Experimental Section). Lifetimes did not vary significantly with change in excitation or emission wavelengths and also did not vary significantly over the 1.2×10^{-6} to 1.2×10^{-3} M range of concentrations of (*E*)-**3** in CH$_2$Cl$_2$, suggesting that self-quenching was unimportant. Above 1.2×10^{-4} M (*E*)-**3** the excitation wavelength (λ_{ex}) had to be shifted from 337 to 375 nm, apparently because of high absorbance at the front face of the 1-cm square cell, which reduced count rates. The lifetime in deoxygenated pentane, $\tau(\lambda_{em}$ 385 nm) = 0.30 ns, increased to 0.53 ns in CH$_2$Cl$_2$ (λ_{em} 420 nm).

For deoxygenated CH$_2$Cl$_2$ as solvent singlet lifetimes of (*E*)-**3** were sufficiently long that the decrease in τ with increasing alcohol concentration could be determined. For MeOH as quencher, measurements could only be made up to 3 M MeOH. A plot of τ^{-1} versus [MeOH] had a slope of $k_q = 1.10 \pm 0.21 \times 10^9$ M^{-1} s^{-1} and an intercept $\tau_o^{-1} = 2.00 \pm 0.35 \times 10^9$ s^{-1} ($R^2 = 0.9508$). From the slope/intercept $k_q\tau = 0.55 \pm 0.21$ M^{-1}, in agreement with the quenching of steady-state fluorescence. TAA was less effective a quencher than MeOH and for a range of concentrations up to 4.0 M, $k_q = 0.364 \pm 0.082 \times 10^9$ M^{-1} s^{-1}, $\tau_o^{-1} = 1.95 \pm 0.20 \times 10^9$ s^{-1} ($R^2 = 0.9312$), and $k_q\tau = 0.19 \pm 0.06$ M^{-1}. The quantitative agreement in $k_q\tau$ values from steady-state fluorescence quenching was thus only fair.

Quantum Yields of Photoproducts. Quantum yields for formation of (*Z*)-**3**, $\Phi(E,Z)$, and hydrosilane (*E*)-**4**, $\Phi(SiH)$, were determined at low conversions with a microoptical bench apparatus at an excitation wavelength of 340 nm, utilizing ferrioxalate actinometry (Experimental Section). In the absence

(12) (a) O'Connor, D. V.; Phillips, D. *Time-correlated Single Photon Counting*; Academic Press: London, 1984. (b) Eaton, D. F. *Pure Appl. Chem.* **1990**, *62*, 1631. (c) Lampert, R. A.; Chewter, L. A.; Phillips, D.; O'Connor, D. V.; Roberts, A. J.; Meech, S. R. *Anal. Chem.* **1983**, *55*, 68. (d) Zimmerman, H. E.; Werthemann, D. P.; Kamm, K. S. *J. Am. Chem. Soc.* **1974**, *96*, 439.

Table 3. Summary of $k_q\tau$ values from plots of $\Phi_f{}^\circ/\Phi_f$ and $\Phi(E,Z)^{-1}$ versus [ROH] and for $\Phi(\text{SiH})^{-1}$ versus $[\text{ROH}]^{-1}$[a]

|		$k_q\tau$/ M^{-1}		
solvent	ROH	$\Phi_f{}^\circ/\Phi_f$ (R^2)[b]	$\Phi(E,Z)^{-1}$ (R^2)[c]	$\Phi(\text{SiH})^{-1}$ (R^2)
pentane	MeOH	0.14 ± 0.01 (0.9763)	0.13 ± 0.02 (0.9932)	0.08 ± 0.02 (0.9953)[d]
CH$_2$Cl$_2$	MeOH	0.54 ± 0.04 (0.9910)	0.47 ± 0.12 (0.9888)	0.47 ± 0.01, 0.55 ± 0.01 (0.9982)[e]
CH$_2$Cl$_2$	TAA	0.08 ± 0.01 (0.9952)	0.10 ± 0.02 (0.9817)	0.08,[f] 0.30 ± 0.09 (0.9456)[g]

[a] Errors are one standard deviation in the fit to a line or curve. [b] From the slope. [c] From slope/intercept. [d] From the intercept/slope. [e] From a quadratic fit, see text. [f] The value from $\Phi_f{}^\circ/\Phi_f$ versus [TAA]. [g] From nonlinear least-squares fit to the data, see text.
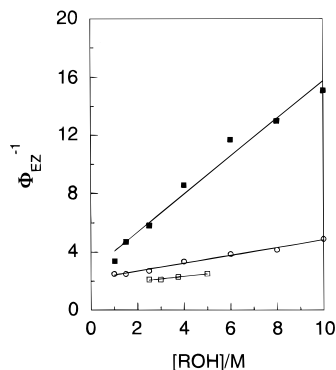
Figure 4. Quenching of the *E,Z* photoisomerization by MeOH in pentane (○), MeOH in CH$_2$Cl$_2$ (■), and TAA in CH$_2$Cl$_2$ (□).

of either MeOH or *tert*-amyl alcohol (TAA) hydrosilane product (*E*)-**4** was not formed in detectable amounts from (*E*)-**3** in pentane, CH$_2$Cl$_2$, or CH$_3$CN. Isomer (*Z*)-**4** proved to be a secondary photoproduct whose yield was negligible at the lower conversions of quantum yield runs. As shown in Table 2, $\Phi(E,Z)$ of (*E*)-**3** decreased by over 30-fold in the polar solvent CH$_3$CN compared to pentane or CH$_2$Cl$_2$. The decrease paralleled the decrease in Φ_f for the same solvents. In contrast, $\Phi(E,Z)$ values for monosilane (*E*)-**5** were constant as the solvent polarity varied.

The *E,Z* photoisomerization of (*E*)-**3** was found to be quenched by alcohols, as shown by the comparison of $\Phi(E,Z)$ without alcohol to $\Phi(E,Z)$ with 5 M MeOH (Table 2). MeOH was a more effective quencher than TAA (Figure 4 and Table 3), and quenching was substantially more pronounced in CH$_2$Cl$_2$ than pentane as solvent. The $k_q\tau$ values of Table 3 correspond to the ratio of slope/intercept of plots of $\Phi^{-1}(E,Z)$ versus [ROH] (Figure 4) and were found to be similar to $k_q\tau$ values obtained from quenching of steady-state fluorescence by ROH (Figure 3).

Quantum yields of hydrosilane (*E*)-**4** increased with increasing alcohol concentration. For pentane as the solvent linear regression analysis of $\Phi^{-1}(\text{SiH})$ versus $[\text{MeOH}]^{-1}$ (Figure 5) gave intercept/slope = $k_q\tau$ similar to values obtained from quenching of steady-state fluorescence and *E,Z* photoisomerization (Table 3). Change in solvent to CH$_2$Cl$_2$ led to a quadratic dependence on $[\text{MeOH}]^{-1}$ (Figure 6). This quadratic behavior was reproduced by two independent, complete sets of experimental data (Experimental Section). From Figure 6 two $k_q\tau$ values could be extracted, either of which matched the $k_q\tau$ values for quenching of both fluorescence and *E,Z* photoisomerization (Table 3). With TAA as the alcohol in CH$_2$Cl$_2$ as solvent, quantum yields $\Phi(\text{SiH})$ were low and covered a very narrow range of values with change in [TAA]. Thus, the TAA points in Figure 5 had considerable scatter, especially at low concentrations of alcohol. Linear regression analysis of the plot (Figure 5) gave intercept/slope = $k_q\tau$ = 0.57, in complete disagreement with quenching of steady-state or time-resolved fluorescence or $\Phi(E,Z)$. The data were thus fit to a nonlinear expression, as described below.
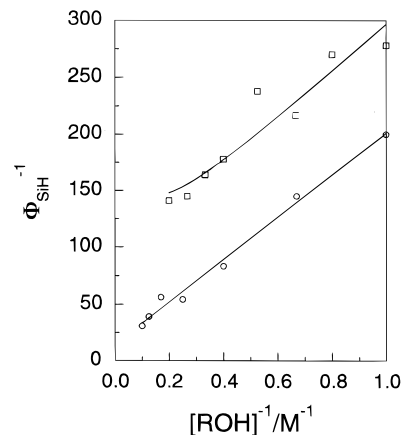
Figure 5. Dependence of quantum yields for hydrosilane (*E*)-**4** on MeOH in pentane (○) and TAA in CH$_2$Cl$_2$ (□).
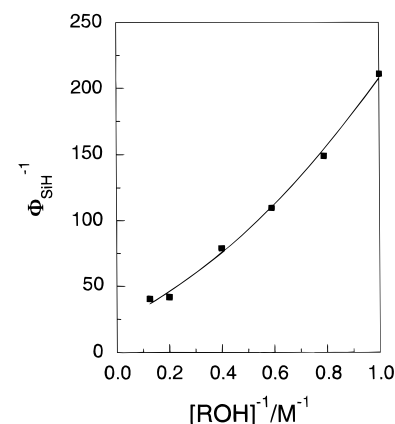
Figure 6. Dependence of quantum yields for hydrosilane (*E*)-**4** on MeOH in CH$_2$Cl$_2$ (■).

Scheme 2
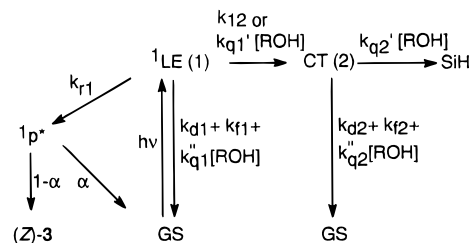
A mechanism must be assumed in order to extract $k_q\tau$ values from the quadratic plot (Figure 6) of $\Phi^{-1}(\text{SiH})$ versus $[\text{MeOH}]^{-1}$ in CH$_2$Cl$_2$. The $k_q\tau$ values in Table 3 are obtained from eq 3, which derives from Scheme 2, taking the rate constant for electron transfer converting the LE to the CT state as $k_{12} \approx k_{q1}'[\text{MeOH}]$. This ROH dependent LE → CT process was proposed previously[1] to account for similar quadratic dependence of $\Phi^{-1}(\text{SiH})$ versus $[\text{EtOH}]^{-1}$ in hexane in the case of aryldisilane **1**. By simple inspection of Figure 6, estimates can be made for parameters *a*, *b*, and *c* in eq 3. Parameters *a* and *b* correspond to $k_q\tau$ values for total quenching of LE and CT

states, respectively (Discussion Section). From the plot the intercept at $x = 0$ is $ab/c = 20-30$. The two points at the lowest [MeOH] provide an estimate for the tangent at 1.0 M MeOH. This estimate is $f'(x) = (a + b)/c + 2x/c = (a + b + 2)/c = 310$ for $x = 1$. If we assume parameter $a = (k_{q1}' + k_{q1}'')\tau_1 = 0.5$ from the fluorescence quenching data (Table 3), then the ratio $[(a + b + 2)/c](ab/c)^{-1}$ gives parameter $b = (k_{q2}' + k_{q2}'')\tau_2 = 0.38-0.62$. A three parameter ($a$, b, c) nonlinear least squares fit of eq 3 to the data gives similar values for parameters a and b in Table 3 and $c = 0.011 \pm 0.003\sigma$.

$$f(x) = \frac{ab}{c} + \frac{(a + b)}{c}x + \frac{1}{c}x^2$$
$$x = [ROH]^{-1}, f(x) = \Phi^{-1}(SiH) \quad (3)$$

$$f(x) = \frac{ab + (a + b)x + x^2}{cx}$$
$$x = [ROH]^{-1}, f(x) = \Phi^{-1}(SiH) \quad (4)$$

Unlike MeOH, TAA has nearly the same $E_T(30)$ as CH_2Cl_2. Thus, the rate of electron transfer converting LE to CT states was taken as a constant k_{12}, independent of ROH. The Scheme 2 mechanism requires the nonlinear expression of eq 4 to hold (Discussion Section). A tangent to the eq 4 curve is $f'(x) = 1/c - ab/cx^2$, and at 1.0 M it has the value $(1 - ab)/c$. If $a = (k_{q1}' + k_{q1}'')\tau_1 = 0.08$ ($k_q\tau$ for fluorescence quenching, Table 3) and $(k_{q2}' + k_{q2}'')\tau_2 = b < 1$, then $1 - ab \approx 1$ and the limiting slope at low concentrations of TAA of $1/c$ will have been nearly reached at 1.0 M TAA. The linear appearance of the plot in Figure 5 can be understood in these terms. By taking $1/c = 186$ (the apparent slope from linear regression analysis of the data), $a = 0.08$, $\Phi^{-1}(SiH) = 278$ at 1.0 M TAA ($x = 1.0$ in eq 4), one can estimate $b = 0.29$. By comparison, the two-parameter nonlinear least-squares fit to the data with $a = 0.08$ fixed (fluorescence quenching) gave $b = 0.30$ (Table 3) and $c = 0.0047 \pm 0.0005\sigma$. Equation 4 will have a minimum at 6.67 M TAA where $\Phi_{max} = 0.0067$. The decrease in quantum yield at higher concentrations of TAA bordering on pure alcohol will be too small to detect experimentally. Our highest concentration of TAA was 5.0 M (1.2:1.0 v/v TAA:CH_2Cl_2), where $\Phi = 0.0070 \pm 0.0010$.

Solvent Polarity Parameters $E_T(30)$ for Binary Solutions of MeOH in CH_2Cl_2. $E_T(30) = N_A(hc/\lambda)$ were calculated from experimental absorption maxima λ of pyridinium-N-phenoxide betaine dye **6** as a function of solute concentration c_p.[11,13,14]

$$Ph \quad Ph$$
$$Ph \overset{+}{N} \quad O^-$$
$$Ph \quad Ph$$

6
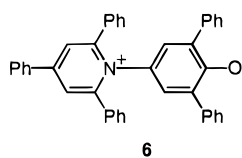
Although $E_T(30) = E_D \ln(c_p/c^* + 1) + E_T°(30)$, the linear relation $E_T(30) = E_D \ln(c_p/c^*) + E_T°(30)$ will, in certain cases, hold for $c^* \ll c_p$ over a wide range of concentrations of polar solute.[11,13b,14] This latter relation was found for 0.30–16 M MeOH in CH_2Cl_2 (Figure 7). From Figure 7 the parameters $c^* = 0.033 \pm 0.008\sigma$ and $E_D = 1.97 \pm 0.065\sigma$; $E_T°(30)$ is 40.7 kcal mol^{-1} for pure CH_2Cl_2. According to Figure 7 a large increase in polarity initially occurs upon addition of small amounts of MeOH, since the apparent intercept at zero [MeOH] has a higher $E_T(30)$ than the pure solvent. This accounts for
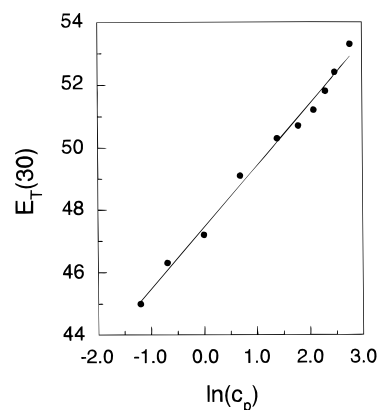
(13) (a) Laurence, C.; Nicolet, P.; Reichardt, C. *Bull. Soc. Chim. Fr.* **1987**, 125. (b) Langhals, H. *New J. Chem.* **1981**, *5*, 97.
(14) Langhals, H. *Angew. Chem., Int. Ed. Engl.* **1982**, *21*, 724.

Figure 7. $E_T(30)$ of binary solutions of MeOH and CH_2Cl_2.

the fact that $\Phi°(E,Z)$ from intercepts of plots of $\Phi^{-1}(E,Z)$ vs [MeOH] in CH_2Cl_2 never equal and are always less than $\Phi°(E,Z)$ measured for pure CH_2Cl_2 (Experimental Section). Relative quantum yields of fluorescence $\Phi_f°/\Phi_f$ determined for the range 1–10 M ROH thus utilized $\Phi_f°$ extrapolated from Φ_f^{-1} versus [ROH].

Triplet Sensitized Photolyses. Irradiation of (*E*)-**3** at 430 nm with 0.050 M biacetyl ($E_T = 56$ kcal mol^{-1}) as triplet sensitizer in CH_2Cl_2 gave (*Z*)-**3** as the sole product. Hydrodimethylsilane **4** was not detected in CH_2Cl_2 or in 5.0 M MeOH in CH_2Cl_2 up to 32% conversion to give product (*Z*)-**3**. At low conversions $\Phi(E,Z) = 0.66$. For these sensitized photolyses the biacetyl absorbed >99.9% of the light.

Discussion

Fluorescence maxima of (*E*)-**3** shift to longer wavelengths with increasing polarity of solvent. Larger shifts are found for CCl_4, $CHCl_3$, and CH_2Cl_2 than for pentane, Bu_2O, Et_2O, and THF, and plots of $\Delta\nu$ versus Δf (eq 1) and ν_f vs $(\epsilon - 1)/(\epsilon + 2)$ (eq 2) show two linear correlations with the halocarbons having the steeper slope (Figure 2). These dual slope plots are suggestive of two emissive excited states. The LE state may be the principal emissive state in ethers. A more polar CT state may contribute significantly to the emission observed halocarbons. The predominance of the LE emission in ethers could be due to complete quenching of the CT component through specific, nucleophilic interaction with electrophilic silicon, which has high affinity for oxygen lone pairs. In the CT state significant charge is expected to be lost from the disilanyl σ electron donor.

From the dual slope plot of Figure 2, the dipole moment, $\mu_e°$, of the solvent-free molecule in the CT state is estimated from eq 2 to be at least 9 D, and the LE state may be at least 6 D, neglecting μ_g in both cases. From an AM1 calculation of (*E*)-**3** with a planar π system and an Si–Si bond perpendicular[15] to the plane of the arene $\mu_g = 4$ D, in which case $\mu_e° = 9$ D for the LE state. The $\Delta\mu$ (eq 1) of 12 and 8 D are somewhat less than the 14.6 and 13.5 D values for the TICT and LE states of 4-cyano-4'-(dimethylamino)stilbene (DCS) and its "stiff stilbene" analog, respectively.[10a] Among the DCS analogs a distinct dual fluorescence is not observed under steady-state conditions, and LE or TICT emissions are observed at similar wavelengths. Dual fluorescence has been observed in time-resolved spectra. The picosecond lifetime experiments show a precursor–successor relationship of short- and long-wavelength emission bands consistent with LE and TICT assignments.[16] However, the long-wavelength band of the time-resolved

(15) Kira, M.; Miyazawa, T.; Mikami, N.; Sakurai, H. *Organometallics* **1991**, *10*, 3793.

experiments is only observed under conditions in which complexation with a second, electronically excited DCS molecule is possible.[16b]

Additional support for the above LE and CT assignments in the case of (*E*)-**3** is provided by comparison of solvatochromic behavior and fluorescence quantum yields with monosilyl cyanostilbene (*E*)-**5**. The solvatochromic slopes (eq 2) for (*E*)-**3** in ethers and for (*E*)-**5** in all solvents are nearly identical (Figure 2). The excited state of (*E*)-**3** we assign as LE (vide supra) in ether solvents thus has similar polarity and displays similar solvatochromic behavior as the emissive excited state of (*E*)-**5**. Apparently a second, more polar excited state does not contribute to the emission of (*E*)-**5** in CH_2Cl_2, and both CH_2Cl_2 and CH_3CN fall on the same correlation line as the ethers in Figure 2. Only small variations in fluorescence quantum yields, Φ_f, of (*E*)-**5** (Table 2) are observed with change in solvent polarity from pentane or CH_2Cl_2 to CH_3CN, whereas for (*E*)-**3** at least an order of magnitude decrease in Φ_f occurs, consistent with conversion of the LE to CT state and quenching of the latter excited state by nucleophilic interaction of the solvent.[1]

As in the case of *trans*-stilbene,[17] the *E,Z* photoisomerizations of (*E*)-**3** and (*E*)-**5** are thought to occur via the twisted $^1p^*$ state. According to Scheme 2, the $^1p^*$ state would be accessed from the LE state and possibly also from the the CT state (not shown in Scheme 2). The LE and CT states may interconvert. Furthermore, intersystem crossing with back electron transfer via the ^{1}CT state could provide a corresponding ^{3}LE pathway for isomerization (not shown in Scheme 2). The disilanyl group of (*E*)-**3** is not expected to exert a significant heavy atom effect that would promote direct intersystem crossing from the ^{1}LE state.[4] In the case of DCS and its analogs the *E,Z* isomerization upon direct photolysis is a singlet photoprocess.[10] The lowest triplet excited state of cyanostilbenes is not populated at room temperature.[18] The rate constant for nonradiative decay in DCS, presumably via the $^1p^*$ state, is known to decrease with increasing polarity of solvent, consistent with selective stabilization of the polar LE and TICT states relative to the less polar $^1p^*$ state.[10,19] The decrease in the nonradiative rate, however, is not mirrored by a significant decrease in quantum yields for *E,Z* photoisomerization with increasing polarity of solvent,[20] whereas a >30 fold decrease in $\Phi(E,Z)$ of (*E*)-**3** occurs in going from pentane to CH_3CN as the solvent (Table 2). By comparison, no decrease in $\Phi(E,Z)$ of (*E*)-**5** is observed in CH_3CN. This difference in behavior between (*E*)-**5** and (*E*)-**3** with increased solvent polarity (vide supra) supports a solvent polarity promoted LE → CT process that competes with the LE → $^1p^*$ photoisomerization (Scheme 1). Nucleophilic quenching of the CT state by CH_3CN would then result in the strong diminution in $\Phi(E,Z)$ and Φ_f (vide supra). $\Phi(E,Z)$ does not decrease in going from pentane to CH_2Cl_2, which suggests the LE-to-CT conversion is partially reversible in the latter solvent in the absence of competitive quenching by alcohol (vide infra).

Linear plots of Φ°_f/Φ_f vs [ROH] are observed (Figure 3) for 1–10 M ROH, consistent with quenching of a single emissive excited state by the alcohol. This suggests only a small contribution is made by the CT state to the composite

fluorescence of (*E*)-**3** in CH_2Cl_2 once 1.0 M ROH is reached. $\Phi^{-1}(E,Z)$ vs [ROH] also shows good linearity (Figure 4), which argues against reaction involving both the ^{1}LE and CT states with both states being quenched by alcohol, i.e., the ^{1}LE → CT → ^{3}LE → $^3p^*$ and ^{1}LE → CT → $^1p^*$ processes. The $k_q\tau$ values for quenching of both the fluorescence and the *E,Z* isomerization by MeOH or *tert*-amyl alcohol (TAA) track each other quite closely (Table 3), regardless of whether the solvent is nonpolar (pentane) or moderately polar (CH_2Cl_2). The two processes thus appear to originate from the same excited state, which we assign as ^{1}LE.

Quantum yields $\Phi(SiH)$ for hydrodimethylsilane (*E*)-**4** increase with increasing concentration of alcohol. The double reciprocal plot for TAA in CH_2Cl_2 appears linear (Figure 5), although the data show scatter due to the low quantum yields observed for (*E*)-**4**, especially at low concentrations of TAA. Nonetheless, the apparent $k_q\tau$ of 0.57 from the ratio intercept/slope from linear regression does not match $k_q\tau$ for quenching of the *E,Z* isomerization or the fluorescence, suggesting that a different excited state is involved in the formation of hydrosilane (*E*)-**4**. The Scheme 2 mechanism for (*E*)-**4** formation involves LE → CT conversion followed by bimolecular reaction of the CT state with TAA. If the LE state is also quenched by TAA, then $\Phi^{-1}(SiH)$ versus $[TAA]^{-1}$ must be nonlinear. Kinetic analysis of Figure 5 (Results Section) indicates such nonlinear behavior will occur in the region corresponding to nearly pure TAA. At lower concentrations of TAA, the Figure 5 plot will be nearly linear. Such behavior follows if quenching of the LE state is relatively inefficient, consistent with $k_q\tau \leq 0.1$ for quenching of *E,Z* photoisomerization and steady-state fluorescence. Inefficient quenching of the LE state of (*E*)-**3** by TAA is furthermore consistent with the absence of a solvent polarity induced LE → CT process, since $E_T(30)$ of TAA ≈ $E_T(30)$ of CH_2Cl_2. On the other hand, change in [MeOH] will change the polarity of the bulk solvent (Figure 7). The plot of $\Phi^{-1}(SiH)$ versus $[MeOH]^{-1}$ will be quadratic, possibly as in Figure 6, if the polarity dependent LE → CT conversion has a rate constant $k_{12} \propto$ [MeOH], as discussed below.

According to the Scheme 2 mechanism $\Phi^{-1}(SiH)$ versus $[TAA]^{-1}$ will follow eq 4. Equation 4 has been derived previously for the analogous case of conversion of an initially populated singlet state to a triplet excited state followed by bimolecular reaction with a quencher to form a product of the excited triplet.[21] In eq 4 $x = [TAA]^{-1}$, $a = k_{q1}\tau_1 = k_{q1}''\tau_1$, $b = k_{q2}\tau_2 = (k_{q2}' + k_{q2}'')\tau_2$, $c = k_{12}\tau_1 k_{q2}'\tau_2$, $\tau_1^{-1} = k_{12} + k_{d1} + k_{r1} + k_{f1}$, and $\tau_2^{-1} = k_{d2} + k_{f2}$. For MeOH in CH_2Cl_2 eq 4 becomes quadratic eq 3 if $k_{12} \approx k_{q1}'$[MeOH] (vide infra), in which case $\tau_1^{-1} = k_{d1} + k_{r1} + k_{f1}$, τ_2^{-1} is the same as for TAA, parameter $a = k_{q1}\tau_1 = (k_{q1}' + k_{q1}'')\tau_1$, $b = k_{q2}\tau_2 = (k_{q2}' + k_{q2}'')\tau_2$, and $c = k_{q1}'\tau_1 k_{q2}'\tau_2$. Parameter a corresponds to the total efficiency of quenching of the LE state and parameter b is the efficiency of quenching of the CT state. Although these efficiencies are high for MeOH as the alcohol (Table 3), such quenching produces hydrosilane (*E*)-**4** inefficiently according to parameter c. Parameter c is the product of the efficiencies of two steps, the LE → CT step, and the step involving nucleophilic cleavage of the Si–Si bond upon reaction of the CT state with the alcohol.

The eq 4 quadratic dependence for $\Phi^{-1}(SiH)$ versus $[ROH]^{-1}$ was previously reported for **1** by Kira and co-workers and was attributed to a rate constant k_{12} that depended upon [ROH].[1] In effect, $k_{12} \propto$ [ROH] was deduced[1] from the behavior of quantum

(16) (a) Gilabert, E.; Lapouyade, R.; Rulliere, C. *Chem. Phys. Lett.* **1988**, *145*, 262. (b) Gilabert, E.; Lapouyade, R.; Rulliere, C. *Chem. Phys. Lett.* **1991**, *185*, 82.

(17) (a) Saltiel, J.; Charlton, J. L. In *Rearrangements in Ground and Excited States*; de Mayo, P., Ed.; Organic Chemistry Series 42; Academic: New York, 1980; Vol. 3, Essay 14. (b) Görner, H.; Kuhn, H. J. *Adv. Photochem.* **1995**, 1.

(18) Görner, H. *J. Photochem.* **1980**, *13*, 269.

(19) Rettig, W.; Majenz, W. *Chem. Phys. Lett.* **1989**, *154*, 335.

(20) Gruen, H.; Görner, H. *Z. Naturforsch.* **1983**, *38*, 928.

(21) (a) Dalton, J. C.; Snyder, J. J. *Mol. Photochem.* **1974**, *6*, 291. (b) If k_{q1}'''[Q] $\neq 0$ and $k_{21} < k_{d2} + k_{f2}$, then eq 5 reduces to the analogous case of bimolecular reaction to give a product of both the singlet and triplet excited state, as derived in ref 21a.

11418 *J. Am. Chem. Soc., Vol. 118, No. 46, 1996*

Liu et al.

yields of fluorescence of **1** as a function of [CH$_2$Cl$_2$] as polar solute in hexane as the solvent. However, the origin of the polar solute effect on k_{12} was ambiguous.

Eisenthal and co-workers[22] found a linear relationship between $\ln(k_{12})$ and the solvent polarity parameter $E_T(30)$. The rate constant k_{12} in this case is the rate constant for electron transfer to form the TICT state in *p*-(dimethylamino)benzonitrile. The linear relationship was attributed to polarity induced barrier height changes rather than viscosity changes on the basis of experiment. Since many binary mixtures follow the relation $\ln(c_p) \propto E_T(30)$ at relatively high concentrations (c_p) of a polar solute in a less polar solvent,[11,13,14] k_{12} will be proportional to c_p for these cases.[3] The linear relationship of $E_T(30)$ versus $\ln(c_p)$ over the entire range of MeOH concentrations in CH$_2$Cl$_2$ used in our study (Figure 7) provides the basis for both $k_{12} \approx k_{q1}'$[MeOH], where k_{q1}' is a proportionality constant, and eq 4.

Equations 3 and 4 for formation of hydrosilane (*E*)-**4** in the binary solvents TAA in CH$_2$Cl$_2$ and MeOH in CH$_2$Cl$_2$ correspond to the special mechanistic case of Scheme 2. A more general mechanism would also include k_{21} to denote the reverse CT(2) → LE(1) process. Also, a sufficiently polar LE(1) state could conceivably give hydrosilane product by reaction with alcohol (k_{q1}'''[Q], Q = ROH) and the CT(2) state could *E,Z* isomerize (k_{r2}). In all cases we assume the LE state is initially populated. By using the steady-state approximation[23] with the more general mechanism, nonlinear eq 5 is obtained for Φ^{-1}(SiH) as a function of [Q] (Q = ROH), $k_{q1} = k_{q1}' + k_{q1}'' + k_{q1}'''$, and $k_{q2} = k_{q2}' + k_{q2}'' + k_{q2}'''$. General eq 5 reduces to

$$\frac{1}{\Phi_{SiH}} = \{(k_{21} + k_{d2} + k_{f2} + k_{r2} + k_{q2}[Q])(k_{d1} + k_{f1} + k_{r1} + k_{q1}[Q]) + k_{12}(k_{d2} + k_{f2} + k_{r2} + k_{q2}[Q])\}/\{k_{q1}'''[Q](k_{21} + k_{d2} + k_{f2} + k_{r2} + k_{q2}[Q]) + k_{12}k_{q2}'[Q]\} \quad (5)$$

eq 4 for TAA in CH$_2$Cl$_2$, if the CT state is the only state giving hydrosilane (*E*)-**4**, i.e., k_{q1}'''[Q] = 0, and if the conversion of the LE to the CT state is irreversible ($k_{21} \ll k_{d2} + k_{f2}$).[21b] As noted above, eq 5 becomes quadratic eq 3 for MeOH in CH$_2$Cl$_2$ when $k_{12} = k_{q1}'$[Q].

According to the general mechanism described above, the quantum yield of *E,Z* photoisomerization, $\Phi^{-1}(E,Z)$, versus [ROH] will correspond to eq 6, which follows from the

$$\frac{1}{\Phi_{EZ}} = \{(k_{r1} + k_{f1} + k_{d1} + k_{q1}[Q])(k_{21} + k_{r2} + k_{f2} + k_{d2} + k_{q2}[Q]) + k_{12}(k_{r2} + k_{f2} + k_{d2} + k_{q2}[Q])/\{(1-\alpha)[k_{r1}(k_{21} + k_{r2} + k_{f2} + k_{d2} + k_{q2}[Q]) + k_{12}k_{r2}] \quad (6)$$

derivation by Wagner for the case of reaction of two excited states that are both quenched.[23] This nonlinear expression simplifies to linear eq 7, if the *E,Z* isomerization occurs primarily

$$\frac{1}{\Phi_{EZ}} = \{(k_{12} + k_{r1} + k_{f1} + k_{d1}) + k_{q1}[Q]\}/\{(1-\alpha)k_{r1}\} \quad (7)$$

in the LE state, and the LE → CT conversion is irreversible. The slope/intercept = $k_{q1}\tau_1 = k_{q1}''\tau_1$ for TAA in CH$_2$Cl$_2$ with τ_1 defined as above in conjunction with eq 3, or slope/intercept = $k_{q1}\tau_1 = (k_{q1}' + k_{q1}'')\tau_1$ for MeOH in CH$_2$Cl$_2$ with τ_1 defined as above in conjunction with eq 4. In addition, if the fluorescence is mainly from the LE state, general eq 8 reduces

(22) Hicks, J.; Vandersall, M.; Babarogic, Z.; Eisenthal, K. B. *Chem. Phys. Lett.* **1985**, *116*, 18.

(23) Wagner, P. J. In *Creation and Detection of the Excited State*; Lamola, A. A., Ed.; Marcel Dekker: New York, 1971; Chapter 4.

to eq 9, where the definition of $k_{q1}\tau_1$ depends on the alcohol and the solvent as with $\Phi^{-1}(E,Z)$ vs [MeOH].

$$\frac{\Phi_f°}{\Phi_f} = [1 + \{k_{f1}k_{q2}[Q]\}/\{k_{f1}(k_{21} + k_{d2} + k_{f2} + k_{r2}) + k_{f2}k_{12}\}]^{-1} \times [1 + \{k_{q1}[Q](k_{21} + k_{d2} + k_{f2} + k_{r2} + k_{q2}[Q]) + k_{q2}[Q](k_{12} + k_{d1} + k_{f1} + k_{r1})\}/\{(k_{d1} + k_{f1} + k_{r1})(k_{21} + k_{d2} + k_{f2} + k_{r2}) + k_{12}(k_{d2} + k_{f2} + k_{r2})\}] \quad (8)$$

$$\Phi_f°/\Phi_f = 1 + k_{q1}\tau_1[Q] \quad (9)$$

In pentane the quantum yields of fluorescence, *E,Z* isomerization, and formation of hydrosilane as functions of [MeOH] all have similar $k_q\tau$ values. The same excited state could be involved in all three photoprocesses, or possibly the conversion of the LE to the CT state becomes reversible. Reversibility over the range of high concentrations of MeOH used in our study seems doubtful unless the CT state in pentane is comparable in energy to the LE state so that $k_{21} \gg k_{q2}[Q]$. In Figure 2 the linear correlations potentially attributable to LE and CT states converge in energy in nonpolar solvents. For the reversible case the general equations reduce to linear eqs 10[23] and 11, where $\chi_1 = k_{21}/(k_{12} + k_{21})$, $\chi_2 = k_{12}/(k_{12} + k_{21})$, and $\tau_e^{-1} = \chi_1(k_{r1} + k_{d1} + k_{f1}) + \chi_2(k_{d2} + k_{f2})$. Our quantum yield data do not distinguish between the two mechanisms in pentane.

$$\frac{1}{\Phi_{E,Z}} = \frac{\tau_e^{-1} + (\chi_1 k_{q1} + \chi_2 k_{q2})[Q]}{(1-\alpha)\chi_1 k_{r1}} \quad (10)$$

$$\frac{1}{\Phi_{SiH}} = \frac{(\chi_1 k_{q1} + \chi_2 k_{q2})}{\chi_2 k_{q2}'} + \frac{1}{\chi_2 k_{q2}' \tau_e[Q]} \quad (11)$$

Conclusion

The *E,Z* photoisomerization of (*E*)-**3** is quenched by MeOH and *tert*-amyl alcohol (TAA). The linear Stern−Volmer plots observed for such quenching are consistent with a single excited state as the reacting state. The quenching constants $k_q\tau$ obtained from these plots parallel those for quenching of the fluorescence of (*E*)-**3** by alcohols, suggesting that the same state that *E,Z* isomerizes is the one that fluoresces. This state is assigned as the LE state, in contrast to the CT assignments of the emissive states of **1**[1] and **2**[2]. The quenching by MeOH is attributed to mainly a solvent polarity induced LE → CT process that competes with the *E,Z* photoisomerization and fluorescence. Strong decreases in $\Phi(E,Z)$ and Φ_f are also observed with change in solvent polarity in going from pentane or CH$_2$Cl$_2$ to CH$_3$CN. The LE → CT process appears to be absent in the monosilylated cyanostilbene (*E*)-**5**. Change in solvent polarity exerts no significant effect on Φ_f and $\Phi(E,Z)$, and these processes can be ascribed to a single excited state, which from solvatochromic plots, has similar polarity as the LE state of (*E*)-**3**. The LE emission of (*E*)-**3** is observed in nonpolar solvents and ethers, which nucleophilically quench the CT contribution to the emission. Otherwise, the fluorescence appears to be a composite of emissions of the LE and CT states in relatively polar nonnucleophilic halogenated solvents. The CT contribution is evident in solvatochromic plots, which show a steeper slope for halogenated solvents than the ethers, which follow a separate linear correlation.

The quadratic behavior previously reported for Φ^{-1}(SiH) versus [ROH]$^{-1}$ in the case of **1**[1] is also observed for hydrosilane (*E*)-**4** formed in binary mixtures of [MeOH] in CH$_2$Cl$_2$ as the

(E)-4-Cyano-4′-(pentamethyldisilanyl)stilbene

J. Am. Chem. Soc., Vol. 118, No. 46, 1996 11419

solvent. The quadratic dependence may be ascribed to an LE → CT process that is promoted by increasing polarity of the solvent with added MeOH. This conclusion is supported by determination of the $E_T(30)$ values for this binary solvent system, which show that the rate constant for electron transfer can be proportional to concentration of alcohol. Reaction of the CT state with alcohol gives hydrosilane (E)-**4** inefficiently, likely due to quenching with deactivation to the ground state. The inefficiency of Φ(SiH) is unlikely to be due to intersystem crossing via back electron transfer of the CT state[4] to generate the triplet stilbene. The triplet is found to E,Z isomerize efficiently, but Φ(E,Z) upon direct photolysis strongly decreases with increasing polarity of solvent. This contrasts with the solvent polarity promoted generation of triplet excited disilanylbenzenes, which results in homolytic cleavage followed by disproportionation of the silyl radical pair.[8] In the case of (E)-**3** the hydrosilane is not detected upon triplet-sensitized photolysis. For the direct photolyses in pure MeOD and mixtures of MeOD in CH_2Cl_2 or pentane SiD labeled hydrosilane (E)-**4** is almost exclusively observed, consistent with the nucleophilic cleavage mechanism, as proposed previously to account for hydrosilane formation from **1**[1] and **2**.[2]

Additional work remains to establish the structure of the intramolecular CT state. Three possible TICT states would have to be considered, one involving C−Si bond rotation and two others involving rotations about C=C−Ar single bonds. Studies of appropriately bridged analogs of DCS show that twisting about the C−N bond is unimportant.[20] The emissive TICT state is instead thought to be produced by rotation of the dimethylanilino group relative to the p-cyanostyryl group. Still another TICT state is possible,[10,16,19] in which the benzonitrile and p-(dimethylamino)styryl groups are mutually orthogonal.[24]

Experimental Section

Spectra were recorded with the following spectrometers: NMR GE GN 300 (300 MHz, ^{1}H, 75 MHz, ^{13}C, 46 MHz, ^{2}H NMR), Perkin-Elmer 320 (UV), Perkin-Elmer LS-5 (fluorescence). A Hewlett-Packard 5890 GC and a HP 5970 mass selective detector were used for GC-MS analyses, which were performed at 70 eV with a DB-1 column (0.25 mm × 30 m, 0.25 μm film thickness), temperature programmed for 150 °C for 5 min and then 250 °C at 10 °C min^{−1}.

Silica gel 60−200 mesh (grade 62, Mallinckrodt) was used for standard column chromatography. Medium pressure liquid chromatography (MPLC) utilized a 82 cm × 2.5 cm column of 230−400 mesh silica gel (grade 9385, 60 A, Aldrich) with ether in hexane as eluant at a flow rate of 15 mL min^{−1}, as specified below. The column was connected to a Gilson Model 305 pump equipped with a 100 mL min^{−1} capacity head, and the eluant was passed through an ISCO UA-5 UV detector.

A Varian 1400 gas chromatograph equipped with flame ionization detector and a HP 3395 electronic integrating recorder was used for analytical separations on a 0.53 mm × 30 m DB-1 capillary column (Megabore) of 1.5 μm film thickness. Nitrogen was the carrier gas. The silanized glass-lined injector was at 250 °C. Detector response was calibrated by standard mixtures.

Solvents were MeOH (EM Omnisolv, distilled from Mg), pentane (Baxter, high purity), hexane (Mallinckrodt), THF (Milsov, refluxed and distilled from sodium and benzophenone), CH_3CN (Aldrich, HPLC, refluxed 3 days over CaH_2 and distilled), CH_2Cl_2 (Aldrich, HPLC, refluxed 3 h over CaH_2 and then distilled), $CHCl_3$ (Fisher, HPLC), Et_2O (Aldrich, distilled from Na), n-Bu_2O (Aldrich, distilled from Na), tert-amyl alcohol (Aldrich, distilled from CaH_2), and CCl_4 (Aldrich).

(E)-4-Cyano-4′-(pentamethyldisilanyl)stilbene, (E)-3. To a solution of 5.0 g (15 mmol) of (E)-4,4′-dibromostilbene[25] in 1000 mL of dry THF at −78 °C was added 9.0 mL (18 mmol) of 2.0 M

n-butyllithium in hexanes, dropwise via syringe, with stirring under nitrogen. A yellow precipitate formed. After the mixture was stirred at −78 °C for 45 min, 3.5 g (21 mmol) of chloropentamethyldisilane[26] was added via syringe, and the mixture was stirred overnight at room temperature. After the addition of 10 mL of water and concentration in vacuo, a standard workup was performed. The residue was extracted by 250 mL of ether and 100 mL of water. The aqueous phase was extracted twice with 100 mL of ether. The combined ether extracts were washed twice with 100 mL of water and once with 100 mL of saturated NH_4Cl and dried over anhydrous Na_2SO_4. The reaction was repeated, and the ether extracts were combined with those of the first reaction and concentrated in vacuo. The colorless solid residue was dissolved in 6 mL of THF and chromatographed on a 90 cm × 2.5 cm column of silica gel eluting with hexane, taking 35-mL fractions. The first six fractions gave 9 g of ca. 60% (E)-4-bromo-4′-(pentamethyldisilanyl)stilbene by GC-MS analysis, along with (E)-4,4′-bis(pentamethyldisilanyl)stilbene (major byproduct) and minor amounts of (E)-4-(pentamethyldisilanyl)stilbene. This mixture was used without further purification for the synthesis of (E)-**3** (vide infra). A small sample purified by MPLC gave the following spectral data: ^{1}H NMR (CDCl$_3$) δ −0.01 (s, 9 H, methyl), 0.26 (s, 6 H, methyl), 6.99 (B part of AB, J = 16.0 Hz, 1 H, vinyl), 7.10 (A part of AB, J = 16.0 Hz, 1 H, vinyl), 7.39−7.51 (m, 8 H, aromatic); GC-MS (70 eV) m/z (relative intensity) 392 (2), 391 (5), 390 (15), 389 (5), 388 (14), 378 (1), 376 (12), 375 (40), 374 (12), 373 (35), 318 (25), 317 (100), 315 (99), 314 (18), 309 (14), 302 (13), 300 (12), 221 (17), 139 (18), 137 (19), 73 (75), 59 (10), 45 (20), 43 (16).

To a solution of 9.0 g (23 mmol) of the above bromostilbene in 250 mL of dry THF at −78 °C was added 15 mL (30 mmol) of 2.0 M n-butyllithium in hexanes via syringe, followed by dropwise addition of 4.2 g (35 mmol) of phenyl cyanate.[27] The reaction mixture was stirred overnight at room temperature. After the above standard workup, but extracting with 200-mL volumes and omitting the NH_4Cl wash, the yellow oily residue was chromatographed on a 90 cm × 2.5 cm column of silica gel (60−200 mesh), initially eluting with hexanes. Once the first component had eluted, the eluant was changed to 3% ether in hexanes and 35-mL fractions were taken. Fractions 20−26 gave 1.5 g of (E)-4-cyano-4′-(pentamethyldisilanyl)stilbene, (E)-**3**, as a light yellow solid, which was purified by MPLC, eluting with 4% ether in hexanes. The middle cut of the peak 130 min retention time gave 1.04 g (10% yield based on 30 mmol of 4,4′-dibromostilbene) of NMR pure product, mp 113−116 °C. (E)-**3** was crystallized 2 to 4 times from 30 mL of 95% EtOH until colorless needles of mp 115−116.5 °C were obtained. The spectral data were as follows: ^{1}H NMR (CDCl$_3$) δ 0.06 (s, 9 H, methyl), 0.35 (s, 6 H, methyl), 7.12 (d, J = 16.1 Hz, 1 H, A part of AB, vinyl), 7.22 (d, J = 16.4 Hz, 1 H, B part of AB, vinyl), 7.48 (d, J = 8.3 Hz, 2 H, A part of AA′BB′, aromatic), 7.49 (d, J = 8.5 Hz, 2 H, B part of AA′BB′, aromatic), 7.60 (d, J = 8.5 Hz, 2 H, A part of AA′BB′, aromatic), 7.63 (d, J = 8.5 Hz, 2 H, B part of AA′BB′, aromatic); ^{13}C NMR (CDCl$_3$) δ −4.2, −2.4, 110.3, 118.9, 126.0, 126.5, 126.7, 132.31, 132.33, 134.1, 136.0, 140.8, 141.7; GC-MS (70 eV) m/z (relative intensity) 337 (4), 336 (11), 335 (32), 334 (6), 322 (3), 321 (8), 320 (24), 264 (6), 263 (24), 262 (100), 261 (13), 246 (4), 205 (3), 204 (3), 203 (4), 131 (3), 130 (3), 103 (3), 75 (3), 74 (6), 73 (60), 59 (18), 58 (3), 53 (5), 45 (19), 44 (4), 43 (18). Anal. Calcd for $C_{20}H_{25}NSi_2$: C, 71.58; H, 7.51. Found: C, 71.63; H, 7.52.

(E)-4-Cyano-4′-(trimethylsilyl)stilbene, (E)-5. (E)-4-Bromo-4′-(trimethylsilyl)stilbene was prepared from 5.0 g (15.0 mmol) of (E)-4,4′-dibromostilbene[25] by a similar procedure as the 4′-(pentamethyldisilanyl) derivative (vide supra), except that 2.1 g (19 mmol) of (chlorotrimethyl)silane was used and the reaction time was shortened to 5 h at room temperature. After standard workup (vide supra) the residue was chromatographed on a 90 cm × 2.5 cm column of silica gel, eluting with hexanes. The first component eluted was 1.9 g (38% yield) of GC-MS pure (E)-4-bromo-4′-(trimethylsilyl)stilbene. The spectral data were as follows: GC-MS (70 eV) m/z (relative intensity) 333 (11), 332 (46), 331 (11), 330 (44), 318 (22), 317 (100), 316 (26),

(24) Lapouyade, R.; Kuhn, A.; Letard, J.-F.; Rettig, W. *Chem. Phys. Lett.* **1993**, *208*, 48.

(25) Bance, S.; Barber, H. J.; Woolman, A. M. *J. Chem. Soc.* **1943**, 1.

(26) Kumada, M.; Yamaguchi, M.; Yamamoto, Y.; Nakajima, J.-I.; Shiina, K. *J. Org. Chem.* **1956**, *21*, 1264.

(27) Murray, R. E.; Zweifel, G. *Synthesis* **1980**, 150.

315 (97), 178 (22), 158 (12), 157 (12), 139 (26), 137 (24), 73 (21), 59 (11), 45 (15), 42 (29).

Cyanostilbene (*E*)-**5** was prepared from 4.0 g (12 mmol) of the above monobromide following a procedure similar to the synthesis of (*E*)-**3** (vide supra). After workup, the yellow residue was chromatographed on a 90 cm × 2.5 cm column, eluting initially with hexanes. Once the first component had eluted, the eluant was changed to 3% ether in hexanes, and further elution gave a light yellow solid. Purification by MPLC eluting with 4% ether in hexanes then gave 0.66 g of NMR pure (*E*)-**5**, which was crystallized from 95% EtOH to give 0.42 g (13% yield based on 12 mmol of monobromide) of colorless needles, mp 142.5−144 °C. The spectral data were as follows: ^{1}H NMR (CDCl$_3$) δ 0.28 (s, 9 H, methyl), 7.10 (d, B part of AB, $J = 16.2$ Hz, 1 H, vinyl), 7.21 (d, A part of AB, $J = 16.2$ Hz, 1 H, vinyl), 7.51 (d, $J = 8.0$ Hz, 2 H, B part of AA′BB′, aromatic), 7.55 (d, $J = 8.0$ Hz, 2 H, A part of AA′BB′, aromatic), 7.59 (d, $J = 8.5$ Hz, 2 H, B part of AA′BB′, aromatic), 7.64 (d, $J = 8.5$ Hz, 2 H, A part of AA′BB′, aromatic); ^{13}C NMR (CDCl$_3$) δ −1.2, 110.7, 119.0, 126.2, 126.9, 132.5, 133.8, 136.6, 141.5, 141.9; GC-MS (70 eV) *m/z* (relative intensity) 277 (26), 263 (24), 262 (100), 204 (5), 203 (7), 131 (9), 73 (5), 59 (12), 43 (17). Anal. Calcd for C$_{18}$H$_{19}$NSi: C, 77.93; H, 6.90; N, 5.05. Found: C, 77.87; H, 6.81; N, 5.19.

(*Z*)-4-Cyano-4′-(trimethylsilyl)stilbene, (*Z*)-5. A mixture of 700 mg (3.93 mmol) of 70% *p*-(trimethylsilyl)benzaldehyde and 1.8 g (3.93 mmol) of (*p*-cyanobenzyl)triphenylphosphonium bromide in 7.1 mmol of lithium methoxide solution (prepared from 50 mg of lithium and 10 mL of MeOH) was stirred for 6 h at room temperature under N$_2$. After workup, the residue was chromatographed on a silica gel column, eluting with 0.5%, 1%, and 2% ether in hexane to afford 300 mg (39%) of GC-MS pure (*E*)-**5** as a colorless solid and 500 mg of a colorless oil, which contained *ca.* 41% (*Z*)-**5** based on GC-MS. Further purification of the oil by MPLC eluting with 0.8% ether in hexane afforded 90 mg (12%) of GC-MS and NMR pure (*Z*)-**5**. The spectral data were as follows: ^{1}H NMR (CDCl$_3$) δ 0.28 (s, 9 H, methyl), 6.58 (d, A part of AB, $J = 12.3$ Hz, 1 H, vinyl), 6.75 (d, B part of AB, $J = 12.0$ Hz, 1 H, vinyl), 7.19 (d, $J = 7.2$ Hz, 2 H, A part of AA′BB′, aromatic), 7.36 (d, $J = 8.7$ Hz, 2 H, A part of AA′BB′, aromatic), 7.42 (d, $J = 7.5$ Hz, 2 H, B part of AA′BB′, aromatic), 7.53 (d, $J = 8.4$ Hz, 2 H, B part of AA′BB′, aromatic); ^{13}C NMR (CDCl$_3$) δ −1.2, 110.4, 118.9, 128.0, 128.4, 129.4, 132.0, 133.2, 133.4, 136.4, 140.4, 142.1; GC-MS (70 eV) *m/z* (relative intensity) 277 (24), 263 (25), 262 (100), 204 (3), 203 (4), 131 (5), 73 (3), 59 (9), 43 (11).

Preparative Direct Photolysis of (*E*)-4-Cyano-4′-(pentamethyl-disilanyl)stilbene, (*E*)-3, in MeOH. A solution of 489 mg (1.46 mmol) of (*E*)-**3** in 250 mL of methanol was purged with nitrogen and then irradiated 15 min through Pyrex with a Hanovia 450-W medium-pressure lamp. GC-MS analyses showed ca. 40% unreacted (*E*)-**3**, ca. 50% of three major photoproducts including (*Z*)-**3** plus the *E* and *Z* isomers of hydrosilane **4**, and ca. 10% of two minor photoproducts, (*E*,*Z*)-4-cyano-4′-(methoxydimethylsilyl)stilbene. The solvent was removed in vacuo and the major products were isolated by MPLC, eluting with 4% ether in hexanes. The cut at the onset of the first peak gave 74 mg (15% yield) of (*Z*)-**3** (retention time 108 min), the middle cut gave 71 mg (18% yield) of (*Z*)-**4** (retention time 120 min), and a later cut gave 204 mg (42%) of unreacted (*E*)-**3** (retention time 136 min). The second peak gave 59.5 mg (16% yield) of (*E*)-**4** (retention time 184 min). MPLC was repeated for each of the three isolated products.

(*Z*)-4-Cyano-4′-(pentamethyldisilanyl)stilbene, (*Z*)-**3**, was crystallized from hexane, mp 58−9 °C. The spectral data were as follows: ^{1}H NMR (CDCl$_3$) δ 0.04 (s, 9 H, methyl), 0.32 (s, 6 H, methyl), 6.56 (d, B part of AB, $J = 12.2$ Hz, 1 H, vinyl), 6.74 (d, A part of AB, $J = 12.2$ Hz, 1 H, vinyl), 7.14−7.51 (m, 8 H, aromatic); ^{13}C NMR (CDCl$_3$) d −2.3, −4.2, 110.4, 119.0, 128.0, 128.3, 129.5, 132.0, 133.4, 133.7, 136.0, 139.8, 142.2; GC-MS (70 eV) *m/z* (relative intensity) 335 (24), 320 (19), 263 (23), 262 (82), 73 (100), 59 (32), 45 (42), 43 (38). Anal. Calcd for C$_{20}$H$_{25}$NSi$_2$: C, 71.58; H, 7.51; N, 4.17. Found: C, 71.85; H, 7.60; N, 4.23.

(*E*)-4-Cyano-4′-(dimethylsilyl)stilbene, (*E*)-**4**, was crystallized from ether in hexane, mp 104−5 °C. The spectral data were as follows: ^{1}H NMR (CDCl$_3$) δ 0.38 (d, $J = 3.7$ Hz, 6 H, methyl), 4.47 (septet, J

= 3.7 Hz, 1 H, silane), 7.12 (d, B part of AB, $J = 16.0$ Hz, 1 H, vinyl), 7.22 (d, A part of AB, $J = 16.0$ Hz, 1 H, vinyl), 7.50−7.65 (m, 8 H, aromatic); ^{13}C NMR (CDCl$_3$) δ −3.9, 110.6, 119.0, 126.2, 126.9, 127.1, 132.3, 132.5, 134.5, 137.0, 138.3, 141.7; GC-MS (70 eV) *m/z* (relative intensity) 263 (49), 249 (17), 248 (82), 170 (28), 145 (30), 121 (20), 105 (12), 103 (12), 59 (28), 58 (53), 53 (24), 51 (11), 45 (28), 44 (14), 43 (100). Anal. Calcd for C$_{17}$H$_{17}$NSi: C, 77.52; H, 6.51; N, 5.32. Found: C, 77.27; H, 6.41; N, 5.30.

The spectral data of (*Z*)-4-cyano-4′-(dimethylsilyl)stilbene, (*Z*)-**4**, were as follows: ^{1}H NMR (CDCl$_3$) δ 0.33 (d, $J = 3.7$ Hz, 6 H, methyl), 4.41 (septet, $J = 3.7$ Hz, 1 H, silane), 6.58 (d, B part of AB, $J = 12.2$ Hz, 1 H, vinyl), 6.74 (d, A part of AB, $J = 12.2$ Hz, 1 H, vinyl), 7.18 (m, B part of AA′BB′, 2 H, aromatic), 7.34 (m, A part of AA′BB′, 2 H, aromatic), 7.43 (m, B part of AA′BB′, 2 H, aromatic), 7.51 (m, A part of AA′BB′, 2 H aromatic); ^{13}C NMR (CDCl$_3$) δ −3.9, 110.5, 118.9, 128.1, 128.6, 129.5, 132.0, 133.1, 134.1, 136.9, 137.3, 142.0; GC-MS (70 eV) *m/z* (relative intensity) 263 (28), 249 (13), 248 (56), 203 (11), 170 (25), 145 (28), 121 (18), 105 (11), 103 (12), 59 (28), 58 (51), 53 (24), 51 (11), 45 (26), 44 (14), 43 (100).

Preparative Direct Photolysis of (*E*)-4-Cyano-4′-(pentamethyl-disilanyl)stilbene in MeOD. A solution of 302 mg (0.9 mmol) of (*E*)-**3** in 150 mL of MeOD (Aldrich, 99.5+% atom D) was purged with nitrogen and then irradiated for 2.5 h with a Hanovia 450-W medium-pressure lamp equipped with a Pyrex filter. GC-MS analyses of aliquots showed that product (*E*)-**4** was 100% monodeuterated, using the parent ion and M − 15 fragment ion to calculate[28] the isotopic distribution. The *m/z* 263 undeuterated ion was absent. (*E*)-4-(Deuteriodimethylsilyl)-4′-cyanostilbene, (*E*)-**4**-d_1, was isolated by MPLC as above for undeuterated (*E*)-**4**. The spectral data were as follows: ^{1}H NMR (CDCl$_3$) δ 0.34 (s, 6 H, methyl), 7.12 (d, B part of AB, $J = 16.4$ Hz, 1 H, vinyl), 7.22 (d, A part of AB, $J = 16.4$ Hz, 1 H, vinyl), 7.50−7.66 (m, 8 H, aromatic); ^{2}H NMR (CDCl$_3$) δ 4.5 (SiD); GC-MS (70 eV) *m/z* (relative intensity) 265 (15), 264 (59), 250 (23), 249 (100), 170 (25), 146 (23), 122 (14), 58 (21), 43 (34).

Photolysis of (*E*)-3 in 5.0 M MeOD in Pentane and CH$_2$Cl$_2$. Solutions of 5% 10^{-3} M (*E*)-**3** in 29 mL of 5.0 M MeOD in pentane or in CH$_2$Cl$_2$ as solvents were purged with nitrogen and then irradiated for 10 min through Pyrex with a Hanovia 450-W medium-pressure lamp. Isotopic compositions of (*E*)-**4** were calculated from the parent and M − 15 fragment ions on GC-MS analyses of aliquots. For pentane the respective ions gave 86% and 91% monodeuteration, and the sample photolyzed with MeOD gave the following data: GC-MS (70 eV) *m/z* (relative intensity) 265 (12), 264 (67), 263 (10), 262 (11), 250 (21), 249 (100), 248 (11), 219 (11), 170 (23), 146 (22), 131 (13), 122 (13), 68 (24), 58 (19), 53 (11), 44 (12), 43 (42), 41 (12). For CH$_2$Cl$_2$ the respective ions gave 94% and 100% monodeuteration and the sample photolyzed with MeOD gave the following data: GC-MS (70 eV) *m/z* (relative intensity) 265 (16), 264 (63), 263 (4), 262 (7), 250 (24), 249 (100), 219 (3), 170 (27), 146 (25), 131 (4), 122 (17), 58 (24), 53 (12), 46 (13), 44 (12), 43 (44), 41 (4).

Fluorescence Spectra of (*E*)-3 and (*E*)-5 in Various Solvents. The fluorescence spectra of ca. 10^{-4} M solutions were measured at the 330 nm excitation wavelength in various solvents (Figure 1 and Table 1). For each of the solvents excitation spectra of (*E*)-**3** obtained at several emission wavelengths were similar to the absorption spectrum; each was red-shifted 30−35 nm due to an artifact of the instrument, as noted previously.[2]

Quantum Yields of Fluorescence of (*E*)-3 and (*E*)-5 in Various Solvents. The fluorescence spectra were measured at the 330 nm excitation wavelength in each solvent at concentrations below 10^{-5} M such that the absorbances were < 0.1. A 1 N H$_2$SO$_4$ solution of quinine bisulfate served as the standard ($\Phi_f = 0.546$).[29a−c] Samples were not deaerated. The quantum yields were calculated from the equation $\Phi_u = [(A_s F_u n_u^2)/(A_u F_s n_s^2)]\Phi_s$,[29d] where Φ is the quantum yield of fluorescence, A is absorbance, Φ is the integrated emission across the

(28) Biemann, K. *Mass Spectrometry*; McGraw-Hill: New York, 1962; p 209.

(29) (a) Meech, S. R.; Phillips, D. *J. Photochem.* **1983**, *23*, 193. (b) Hamai, S.; Hirayama, F. *J. Phys. Chem.* **1983**, *87*, 83. (c) Melhuish, W. H. *J. Phys. Chem.* **1961**, *65*, 229. (d) Eaton, D. F. In *Handbook of Organic Photochemistry*; Scaiano, J. C., Ed.; CRC Press: Boca Raton, 1989; Vol. I, Chapter 8.

band, n is the refractive index of the solvent, u stands for unknown, and s pertains to standard. The Φ_f values are summarized in Table 2.

Relative Quantum Yields of Fluorescence of (*E*)-3 in Pentane and CH₂Cl₂ versus [MeOH] and [*tert*-Amyl Alcohol]. Fluorescence spectra of 0.01 M solutions of (*E*)-3 were measured at the 330 nm excitation wavelength in each solvent at various concentrations of alcohol. The integrated area under the fluorescence peak was considered proportional to Φ_f, and Φ_f° was obtained by extrapolation to zero [ROH]. The data are plotted in Figure 3 and summarized in Table 3.

The data for MeOH in pentane were as follows: Φ_f°/Φ_f ([MeOH]/ M), 1.00 (0.0), 1.14 (1.0), 1.33 (2.0), 1.52 (4.0), 1.86 (6.0), 1.89 (8.0), 2.55 (10.0). Linear regression analysis of Φ_f°/Φ_f vs [MeOH] has a slope $k_q\tau = 0.14 \pm 0.01$ ($R^2 = 0.9763$).

The data for MeOH in CH₂Cl₂ were as follows: Φ_f°/Φ_f ([MeOH]/ M), 1.00 (0.0), 1.65 (1.0), 1.93 (2.0), 3.13 (4.0), 4.62 (6.0), 5.06 (8.0), 5.25 (10.0). Linear regression analysis (omitting the 10 M point) of Φ_f°/Φ_f vs [MeOH] has a slope $k_q\tau = 0.54 \pm 0.04$ ($R^2 = 0.9910$).

The data for *tert*-amyl alcohol (TAA) in CH₂Cl₂ were as follows: Φ_f°/Φ_f ([TAA]/M), 1.00 (0.0), 1.11 (1.0), 1.18 (2.0), 1.24 (3.0), 1.32 (4.0), 1.43 (5.0). Linear regression analysis of Φ_f°/Φ_f vs [TAA] has a slope $k_q\tau = 0.08 \pm 0.01$ ($R^2 = 0.9952$).

Relative Quantum Yields of Fluorescence of (*E*)-4-Cyano-4′- (trimethylsilyl)stilbene (*E*)-5 in Pentane versus [MeOH]. The fluorescence spectra of 1×10^{-4} M solutions of (*E*)-5 were measured at the 330 nm excitation wavelength in pentane for various concentrations of MeOH, as described above. The data were as follows: Φ_f°/ Φ_f ([MeOH]/M), 1.00 (0.0), 1.60 (2.0), 1.62 (4.0), 2.00 (6.0), 2.20 (8.0), 2.68 (10.0). Linear regression analysis of Φ_f°/Φ_f vs [MeOH] has a slope $k_q\tau = 0.15 \pm 0.02$ ($R^2 = 0.9780$).

Single Photon Counting Lifetime Instrument. The instrument was constructed from standard components according to the literature.[12] Excitation pulses of 1.2 ns fwhm were provided by a nF-900 nanosecond flashlamp (Edinburgh Analytical Instruments) filled with nitrogen (0.5 bar) and controlled by a nF900 power supply unit. A synchronization photomultiplier was connected to the flashlamp discharge chamber by a glass fiber optic cable and provided the start signal via a constant fraction discriminator (CFD, Ortec 583) for triggering the time-to-amplitude converter (TAC, Ortec 566). Excitation was focused on the slits of an excitation monochromator. Single photon emission was monitored at 90° by a Hamamatsu 1527 blue sensitive phototube (STOP PMT) via an emission monochromator. Samples were contained in 1-cm-square long-necked Pyrex cells with provision for freeze−pump−thaw or nitrogen purge. The signal from the STOP PMT was fed via a 11.5-ns delay (calibrated variable delay box, Ortec 463) to a CFD (Ortec 583) into the STOP input of the TAC. A Norland Model 5000 MCA card housed in a PC was connected to the output of the TAC and counts were stored in 1024 channels. FLA 900 analysis software (ver 3.66) provided the nonlinear least-squares reconvolution method for obtaining the decay function from the sample profile and instrument response function (lamp profile from Ludox). The χ^2 test and the Durbin-Watson (DW) parameter[12b] were used as statistical tests to judge the quality of fitted decays.

Singlet Excited State Lifetime Determinations of (*E*)-3. Samples were purged with nitrogen for 30 min and sealed by Teflon stopcock. Unless noted otherwise, the excitation wavelength was 337 nm. The flashlamp was operated at 50 kHz repetition rate. Sample acquisition rate was monitored by a HP5216A counter and kept <5% by adjusting lamp iris and excitation monochromator slits. Acquisition was stopped when the maximum counts in a channel reached 2000. Instrument response (lamp profile) was measured under identical conditions as the sample, but with $\lambda_{ex} = \lambda_{em}$ using Ludox (34 wt% suspension in water, Aldrich). Satisfactory monoexponential fits of decays were obtained. Anthracene was used to test and check the calibration of the instrument.[12c]

Lifetimes at an emission wavelength of 420 nm were measured for concentrations of (*E*)-3 ranging from 1.2×10^{-6} to 1.2×10^{-3} M in CH₂Cl₂ as the solvent. At high concentrations the excitation wavelength was increased to 375 nm to compensate for decreased count rates, apparently due to front surface absorption of the sample. The results were as follows [τ/ns (concentration of (*E*)-3/M, χ^2, DW)]: 0.47 (1.19 $\times 10^{-6}$, 1.28, 1.92), 0.32 (1.19 $\times 10^{-6}$, 1.20, 1.82), 0.45 (5.97 $\times 10^{-6}$, 1.10, 1.84), 0.50 (5.97 $\times 10^{-6}$, 1.20, 1.92), 0.60 (1.19 $\times 10^{-5}$, 1.30,

1.74), 0.53 (1.19 $\times 10^{-5}$, 1.09, 1.72), 0.52 (5.97 $\times 10^{-5}$, 1.15, 1.79), 0.59 (5.97 $\times 10^{-5}$, 1.27, 1.61), 0.55 (1.19 $\times 10^{-4}$, 1.20, 1.69), 0.52 (1.19 $\times 10^{-4}$, 1.21, 1.81), 0.53 (5.97 $\times 10^{-4}$, 1.16, 1.91, $\lambda_{ex} = 375$ nm), 0.49 (5.97 $\times 10^{-4}$, 1.20, 1.87, $\lambda_{ex} = 375$ nm), 0.49 (1.19 $\times 10^{-3}$, 1.19, 1.65, $\lambda_{ex} = 375$ nm), 0.53 (1.19 $\times 10^{-3}$, 1.15, 1.71, $\lambda_{ex} = 375$ nm).

Lifetimes τ (λ_{em} 420 nm) for 1.19×10^{-5} M solutions of (*E*)-3 in CH₂Cl₂ at various concentrations of MeOH were as follows [τ/ns ([MeOH]/M, χ^2, DW)]: 0.60 (0.0, 1.30, 1.74), 0.53 (0.0, 1.09, 1.72), 0.30 (0.5, 1.15, 1.90), 0.35 (0.5, 1.17, 1.91), 0.34 (1.0, 1.12, 1.79), 0.22 (1.0, 1.14, 1.80), 0.30 (2.0, 1.25, 1.71), 0.25 (2.0, 1.22, 1.76), 0.17 (3.0, 1.11, 1.81), 0.19 (3.0, 1.17, 1.91), from linear regression analysis of τ^{-1} vs [MeOH] the slope/intercept = $k_q\tau = 0.55 \pm 0.21$ ($R^2 = 0.9508$).

Lifetimes τ (λ_{em} 420 nm) for 1.19×10^{-5} M solutions of (*E*)-3 in CH₂Cl₂ at various concentrations of TAA were as follows [τ/ns ([TAA]/ M, χ^2, DW)]: 0.60 (0.0, 1.30, 1.74), 0.53 (0.0, 1.09, 1.72), 0.32 (1.0, 1.13, 1.85), 0.47 (1.0, 1.20, 1.75), 0.42 (1.0, 1.16, 1.77), 0.41 (1.0, 1.14, 1.81), 0.32 (2.0, 1.11, 1.80), 0.47 (2.0, 1.13, 1.76), 0.40 (2.0, 1.13, 1.84), 0.43 (2.0, 1.13, 1.83), 0.25 (3.0, 1.17, 1.78), 0.32 (3.0, 1.12, 1.82), 0.34 (3.0, 1.11, 1.91), 0.32 (3.0, 1.12, 1.88), 0.28 (4.0, 1.10, 1.93), 0.31 (4.0, 1.16, 1.83), 0.36 (4.0, 1.20, 1.93), 0.30 (4.0, 1.24, 1.90), linear regression analysis of τ^{-1} vs [TAA] gave slope/ intercept = $k_q\tau = 0.19 \pm 0.06$ ($R^2 = 0.9312$).

General Procedure for Quantum Yield Determinations of Photolyses of (*E*)-3 and (*E*)-5. A semimicrooptical bench for quantum yield determinations was constructed along the lines specified by Zimmerman.[30a] Light from a 200-W high-pressure mercury lamp was passed through an Oriel monochromator set at 340 nm with 3-mm entrance and exit slits to give a 20 nm bandpass fwhm, collimated through a lens, and split by a beam splitter to divert 17% of the light to a cell containing an actinometer, perpendicular to the light path. The photolysate in a 5 cm × 1.8 cm quartz cylindrical cell of 12.5-mL volume was mounted in line with the optics, monochromator and lamp. Light output was monitored by ferrioxalate actinometry,[30b] using the splitting ratio technique.[30a]

(*Z*)-3 and (*Z*)-5 were quantified by GC analyses of photolysates. (*E*)-4 was quantified after concentration in vacuo and dissolution in ca. 2 mL of CH₂Cl₂. Retention times at 210 °C for photolysates of (*E*)-3 were as follows: *n*-docosane (Aldrich, internal standard), 17.9 min; (*E*)-4, 26.8 min; (*Z*)-3, 29.4 min; (*E*)-3, 79.7 min. Retention times at 220 °C for photolysates of (*E*)-5 were as follows: (*Z*)-5, 12.9 min; *n*-docosane, 15.9 min; (*E*)-5, 26.2 min.

Quantum Yields in Various Solvents. Data for photolyses of 0.01 M (*E*)-3 were as follows: $\Phi(E,Z)$ (pentane), 0.410; $\Phi(E,Z)$ (CH₂Cl₂), 0.552; $\Phi(E,Z)$ (CH₃CN), 0.012. Data for photolyses of 0.01 M (*E*)-5 were as follows: $\Phi(E,Z)$ (pentane), 0.382; $\Phi(E,Z)$ (CH₂Cl₂), 0.403; $\Phi(E,Z)$ (CH₃CN), 0.391.

Quantum Yields in Pentane Containing MeOH. Data for photolysis of 0.01 M (*E*)-3 were as follows: $\Phi(E,Z)$ ([MeOH]/M) 0.399 (1.0), 0.399 (1.5), 0.369 (2.5), 0.298 (4.0), 0.258 (6.0), 0.240 (8.0), 0.203 (10.0); linear regression analysis of $\Phi^{-1}(E,Z)$ vs [MeOH] (Figure 4) gave slope/intercept = $k_q\tau = 0.13 \pm 0.02$ ($R^2 = 0.9932$; Table 3) and from the intercept $\Phi^\circ(E,Z) = 0.465$ compared to measured $\Phi^\circ(E,Z) = 0.410$ without MeOH. $\Phi(SiH)$ ([MeOH]/M), 0.0050 (1.0), 0.0069 (1.5), 0.012 (2.5), 0.018 (4.0), 0.018 (6.0), 0.026 (8.0), 0.033 (10.0); linear regression analysis of $\Phi^{-1}(SiH)$ vs [MeOH]$^{-1}$ (Figure 5) gave intercept/slope = $k_q\tau = 0.08 \pm 0.02$ ($R^2 = 0.9953$; Table 3).

Quantum Yields in CH₂Cl₂ Containing MeOH. Data for photolysis of 0.01 M (*E*)-3 were as follows: $\Phi(E,Z)$ ([MeOH]/M), 0.295 (1.0), 0.212 (1.5), 0.172 (2.5), 0.117 (4.0), 0.086 (6.0), 0.077 (8.0), 0.066 (10.0); linear regression analysis $\Phi^{-1}(E,Z)$ vs [MeOH] (Figure 4) gave slope/intercept = $k_q\tau = 0.47 \pm 0.12$ ($R^2 = 0.9888$; Table 3), and from the intercept $\Phi^\circ(E,Z) = 0.362$ compared to measured $\Phi^\circ(E,Z) = 0.582$ without MeOH. Data for $\Phi(SiH)$ ([MeOH]/M) were as follows: 0.0043 (1.0), 0.0079 (1.5), 0.015 (2.5), 0.017 (4.0), 0.025 (6.0), 0.031 (8.0), 0.029 (10.0); quadratic fit of $\Phi^{-1}(SiH)$ vs [MeOH]$^{-1}$ to eq 3 was obtained with parameters $a = 0.40 \pm 0.01$, $b = 0.44 \pm 0.01$, and $c = 0.0088 \pm 0.0027$ ($R^2 = 0.9967$). A second set of data

(30) (a) Zimmerman, H. E. *Mol. Photochem.* **1971**, *3*, 281. (b) Hatchard, C. G.; Parker, C. A. *Proc. R. Soc. London* **1956**, *235*, 518.

were obtained from a photolysis in which the internal standard amount and analytical conditions were optimized for (*E*)-**4** and $\Phi(E,Z)$ was not determined; data for $\Phi(SiH)$ ([MeOH]/M) were as follows: 0.0047 (1.0), 0.0067 (1.3), 0.0091 (1.7), 0.013 (2.5), 0.024 (5.0), 0.025 (8.0); quadratic fit of $\Phi^{-1}(SiH)$ vs [MeOH]$^{-1}$ (Figure 6) to eq 3 was obtained with parameters $a = 0.55 \pm 0.01$, $b = 0.47 \pm 0.01$, $c = 0.011 \pm 0.002$ ($R^2 = 0.9982$, Table 3).

Quantum Yields in CH₂Cl₂ Containing MeOH and Ferrocene. The *E,Z* photoisomerization and formation of (*E*)-**4** were not quenched by 5×10^{-4} M added ferrocene. Data for photolysis of 0.01 M (*E*)-**3** were as follows: $\Phi(E,Z)$ ([MeOH]/M), 0.275 (1.0), 0.232 (1.5), 0.176 (2.5), 0.125 (4.0), 0.097 (6.0), 0.079 (8.0), 0.062 (10.0); linear regression analysis of $\Phi^{-1}(E,Z)$ vs [MeOH] gave slope/intercept = $k_q\tau = 0.59 \pm 0.15$ ($R^2 = 0.9987$), and from the intercept $\Phi°(E,Z) = 0.434$ compared to measured $\Phi°(E,Z) = 0.633$ at zero MeOH. Data for $\Phi(SiH)$ ([MeOH]/M) were as follows: 0.0044 (1.0), 0.0077 (1.5), 0.014 (2.5), 0.018 (4.0), 0.028 (6.0), 0.029 (8.0), 0.029 (10.0); quadratic fit of $\Phi^{-1}(SiH)$ vs [MeOH]$^{-1}$ to eq 3 was obtained with parameters $a = 0.41 \pm 0.01$, $b = 0.46 \pm 0.01$, $c = 0.009 \pm 0.002$ ($R^2 = 0.9989$).

Quantum Yields in CH₂Cl₂ Containing *tert*-Amyl Alcohol (TAA). Data for photolysis of 0.01 M (*E*)-**3** were as follows: $\Phi(E,Z)$ ([TAA]/M), 0.475 (2.5), 0.474 (3.0), 0.436 (3.75), 0.399 (5.0); linear regression analysis of $\Phi^{-1}(E,Z)$ vs [TAA] (Figure 4) gave slope/intercept ratio $k_q\tau = 0.10 \pm 0.02$ ($R^2 = 0.9817$; Table 3) and from the intercept $\Phi°(E,Z) = 0.610$ compared to measured $\Phi°(E,Z) = 0.522$ without TAA. Data for $\Phi(SiH)$ ([TAA]/M) were as follows: 0.0036 (1.0), 0.0037 (1.25), 0.0046 (1.5), 0.0042 (1.9), 0.0056 (2.5), 0.0061 (3.0), 0.0069 (3.75), 0.0071 (5.0); nonlinear fit of $\Phi^{-1}(SiH)$ vs [TAA]$^{-1}$ (Figure 5)

to eq 4 was obtained with parameters $a = 0.08$ (fixed), $b = 0.30 \pm 0.09$, $c = 0.0047 \pm 0.0005$ ($R^2 = 0.9456$; Table 3).

Quantum Yields in CH₃CN Containing 5.0 M MeOH. Photolysis of 0.01 M (*E*)-**3** in CH₃CN containing 5.0 M MeOH gave $\Phi(E,Z) = 0.012$ and $\Phi(SiH) = 0.014$.

Triplet Sensitized Photolyses of (*E*)-3 in CH₂Cl₂ with 0.050 M Biacetyl as Sensitizer. The photolyses followed the general procedure for quantum yields. Irradiation was at 430 nm such that the biacetyl sensitizer absorbed >99.9% of the light. (*Z*)-**3** was the only product detected in CH₂Cl₂ or in 5.0 M MeOH in CH₂Cl₂ up to 32% conversion. No (*E*)-**4** was detected. At low conversions $\Phi(E,Z) = 0.66$ in CH₂Cl₂.

Solvent Polarity Parameters $E_T(30)$ for Binary Mixtures of MeOH in CH₂Cl₂. The $E_T(30)$ values were determined following the experimental procedures described in the literature.[11,13,14] The absorption maxima λ_{max} of 10^{-4} M solutions of pyridinium-*N*-phenoxide betaine dye **6** (see Results section) in CH₂Cl₂ were measured for various concentrations of MeOH. The results (Figure 7) were as follows: λ_{max}/nm ([MeOH]/M), 636 (0.3), 618 (0.5), 606 (1.0), 582 (2.0), 568 (4.0), 564 (6.0), 558 (8.0), 552 (10.0), 546 (12.0), 536 (16.0). The $E_T(30)$ values were calculated as described in the Results section.